Scaling Behavior of Anisotropic Organic Thin Films Grown in High Vacuum

F. Biscarini, P. Samorí, O. Greco, and R. Zamboni

CNR-Istituto di Spettroscopia Molecolare, Via P. Gobetti 101, 40129 Bologna, Italy

(Received 7 August 1996)

Roughness scaling properties of sexithienyl thin films are investigated by scanning force microscopy as a function of the substrate deposition temperature. The correlation length of the surface fluctuations follows the behavior of the average domain size, increasing exponentially with temperature from submicron to micron scales. Self-affinity is exhibited on 3 orders of magnitude of the spatial frequencies when the morphology changes from grain aggregates to lamellae. The decay with temperature of the roughness scaling exponent α from 1 to 0.7 suggests a transition from diffusion-limited growth to a strong adsorption regime. [S0031-9007(97)02761-0]

PACS numbers: 61.43.Hv, 61.16.Ch, 73.61.Ph, 78.66.Qn

Interfaces grown under nonequilibrium conditions exhibit an apparently irregular geometry that can be analyzed in terms of the scaling properties of the surface fluctuations [1]. An intense theoretical activity based on continuum as well as discrete growth models has provided scaling relations between roughness (i.e., the mean square fluctuation) and thickness of the growing interface, and upon the change of the spatial scale of observation in the experiment. Structures that preserve a similar morphology upon a change of magnification and after a rescaling of the third dimension (z axis) are termed self-affine, and they play a central role in the theories of growth. For a self-affine surface, roughness scaling follows simple power laws with a growth exponent β and a scaling exponent α, which unambiguously distinguish the growth universality class. The substrate temperature during deposition changes continuously the scaling parameters and a new type of roughening transition should occur due to crossover between different processes [2,3]. Techniques such as gas adsorption [4], x-ray reflectivity [4,5], low-energy electron diffraction [6], optical scattering [7], and scanning probe microscopy (SPM) [7–13] probe the surface scaling behavior and provide evidence for the predictions of growth theories. SPM techniques are particularly convenient for the direct investigation of the surface roughness on a wide range of spatial lengths, and several methods of analysis of SPM images have been proposed which use direct space data [8–10] or their Fourier transform [7,11–13]. The effort has been mainly focused on the study of the growth of metal and semiconductor thin films [8–12]. In the field of polymer films there are few systematic works at this time [13,14]. On the other hand, there has not been an extensive investigation to date of roughness scaling behavior in molecular films grown in high vacuum, despite the wide interest in the fundamental aspects and applications of charge and energy transport in these systems [15]. Little is known on the evolution of a growing interface formed by anisotropic molecules, and on the influence of orientational degrees of freedom, anisotropic interactions, and steric factors upon the scaling relations predicted by kinetic growth theories. This information would be important in order to understand the mechanism by which molecular films grow and how to control interfacial properties which are relevant to much of the physics of these systems.

In this Letter we discuss a change of morphology in van der Waals anisotropic films which might be related to a kinetic roughening transition. We focus on sexithienyl (T6), a rigid rodlike conjugated molecule with peculiar self-organization and transport properties which make it an interesting prototype for studying the physics of molecular devices [16]. In our experiment the films are grown on ruby mica by high-vacuum sublimation (base pressure 10^{-6}–10^{-7} mbar). The substrate temperature during the deposition is the experimental variable, while film thickness (100 nm) and deposition rates (0.2–1 Å/s) monitored by a quartz oscillator are kept constant within the experimental reproducibility [17]. T6 films are highly ordered and exhibit uniaxial symmetry with the molecules tilted at 0°–30° angle from the surface normal and stacking in parallel layers. Between 22 and 265 °C the size of the ordered domains increases and slight changes in the interlayer spacing occur [18]. Our aim is to elucidate the effect of the deposition temperature on the film roughness scaling behavior.

The film morphology on a wide range of scan lengths (from 50 μm down to 2μm, and for a few samples from 1 μm down to 200 nm) has been investigated by scanning force microscopy (SFM) operated in contact mode [17]. At temperatures below 200 °C the film consists of grains, while above 200 °C the aggregate is made of large anisotropic lamellae (Fig. 1). The grain aggregates do not appear similar up on magnification although an underlying texture (resembling cauliflowerlike structures) is resolved within large grains [Figs. 1(a) and 1(b)]. On the other hand, the lamellar structure in high-temperature aggregates appears on a wide range of scale lengths, and some characteristic lengths relative to the scan size are preserved upon different magnification [Figs. 1(c) and 1(d)]. This suggests that T6 films evolve towards a self-affine topology as the morphology changes from grains to lamellae.

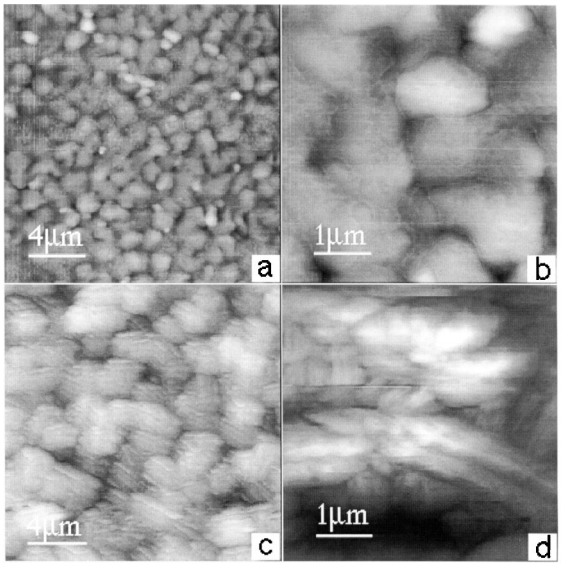

FIG. 1. SFM images of T6 films. At $T = 150\,^{\circ}\mathrm{C}$: (a) scan length $L = 20\ \mu$m, height range $h = 150$ nm; (b) $L = 5\ \mu$m, $h = 130$ nm. At $T = 200\,^{\circ}\mathrm{C}$: (c) $L = 20\ \mu$m, $h = 490$ nm; (d) $L = 5\ \mu$m, $h = 350$ nm. Grey scale ranges from 0 (black) to the height value h (white). Contrast is enhanced by modifying the transfer curve between grey levels and height.

We analyze the scaling behavior of the SFM topographical profiles using their power spectral density (PSD) [7,11–13]

$$\mathrm{PSD}(f) = \frac{1}{L}\left|\int_0^L dx\, h(x) e^{i2\pi f x}\right|^2. \qquad (1)$$

Here $h(x)$ is the apparent topographical height with respect to the mean height ($\langle h\rangle = 0$) calculated on images with scan size L, x is the fast scan direction, and f is the spatial frequency. A self-affine structure exhibits a power-law decay $\mathrm{PSD}(f) = K_0 f^{-\gamma}$ in a finite range of f. The roughness scaling exponent α is related to γ by $\alpha = (\gamma - d)/2$ where the line scan dimension d equals 1 in our case. Our analysis is performed on raw data 400×400 pixel images which are corrected for trends by removal of the best-fit plane. For each image, fast Fourier transform algorithm is applied to each scan line to estimate a 256-frequency point PSD and single-line PSD's are averaged. Finally, representative PSD are obtained by averaging the logarithmic spectra of 3–8 images of different sample zones and cropping together spectra at different scan lengths in order to account evenly for all relevant spatial features. Spectra which deviate considerably from "typical" ones are rejected as explained in Refs. [7,17]. For each scan length L, the spatial frequencies range between $1/L$ and the Nyquist frequency $256/L$. Thus, for 5 μm scan size it is possible to access information on scale lengths comparable to the tip radius of curvature (30–50 nm), which sets the intrinsic high-frequency cutoff of the technique.

The PSDs in Fig. 2 exhibit two distinct regions: (i) a plateau PSD ($1/L$) at low spatial frequencies (white spectrum) denoting the absence of nonlocal correlations along the line scans, and (ii) a frequency-dependent decaying branch. The steeper portion of the latter is taken as the self-affine range, while the high-frequency range with a smaller slope is discarded since it is more affected by noise and aliasing. The range of the intersection between the self-affine branch and the plateau defines the inverse of the correlation length ξ:

$$\xi = \exp\left\{\frac{\ln[\mathrm{PSD}(1/L)] - \ln K_0}{\gamma}\right\}. \qquad (2)$$

Figure 3(a) shows that ξ increases exponentially vs the inverse temperature with an activation energy $E_A = 0.13 \pm 0.02$ eV. We fit ξ vs the experimental mean area $\langle A\rangle$ of the domains reported in Ref. [17] to yield $\langle A\rangle \xi^{2.4(\pm 0.5)}$. Therefore, we show that within the experimental error the correlation length is proportional to the effective radius of

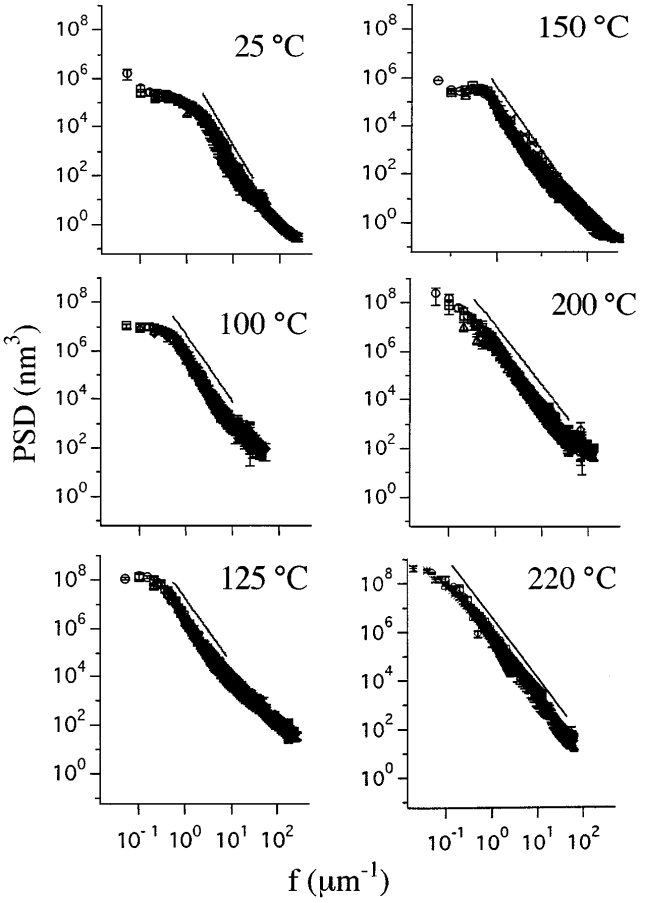

FIG. 2. Evolution of the power spectral density (PSD) vs spatial frequency as a function of the deposition temperature. The mean absolute error estimated by averaging spectra from several images is reported as the error bar, and its inverse is taken as a weight in the fitting of the decaying branch. Best-fit lines with parameters K_0 and γ are shown within the self-affine data range.

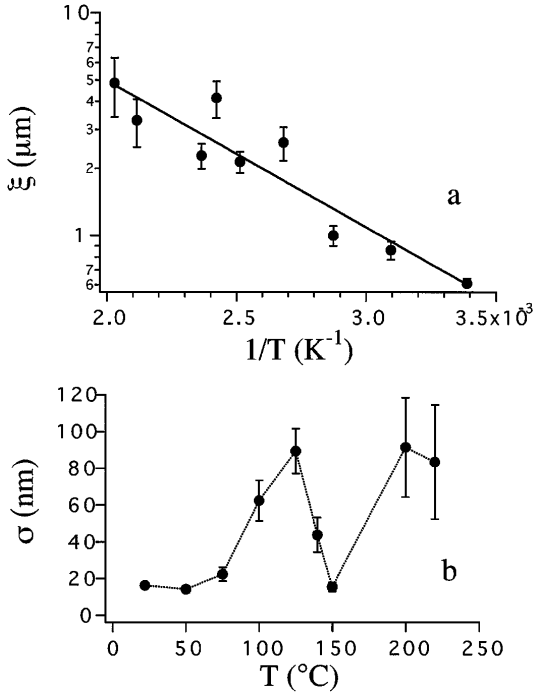

FIG. 3. (a) Correlation length vs inverse substrate temperature. Weighted best-fit Arrhenius equation $\xi(\mu\mathrm{m}) = \exp[4.6(\pm 0.6) - 1.5(\pm 0.2) \times 10^3/T(\mathrm{K})]$ is plotted as the solid line. (b) Saturation roughness estimated from Eq. (3) vs substrate temperature during deposition. The dotted line is a guide for the eye. Error bars are estimated by propagation of errors from Eqs. (2) and (3), respectively.

the domain and this framework allows one to estimate the average domain size independently on arbitrary statistical sampling. The large error on the exponent might be a consequence of the stability of the data and our level of analysis. In fact, the domain size is gamma-distributed so that the statistical uncertainty grows linearly with $\langle A \rangle$ [17]. Furthermore, 1D PSD analysis might underestimate ξ in the anisotropic samples when compared to a more rigorous angular averaging of the 2D power spectra [7]. To overcome the problem of preferential stretching directions and to obtain a coarse but effective rotational averaging, we have always imaged randomly oriented samples with respect to the fast scan direction.

The low-frequency plateau PSD$(1/L)$ is related to the saturation roughness σ (which represents the fluctuations on large scale lengths) by the Wiener-Kintchine theorem. We obtain an approximate expression for σ^2 by first modeling the PSD as piecewise, viz. plateau + self-affine branch, then by integrating the PSD between $1/L$ and the high-frequency limit of the self-affine branch, $f_{\max}$:

$$\sigma^2(L) \approx \mathrm{PSD}\left(\frac{1}{L}\right)\left[\frac{\gamma}{(\gamma - 1)}\,\frac{1}{\xi} - \frac{1}{L}\right]. \qquad (3)$$

Here it has been neglected a term within bracket of the order of $(\xi f_{\max})^{1-\gamma}$, and since $\xi f_{\max} \approx 10\text{–}10^3$ and $\gamma \approx 2.5\text{–}3$, then the relative error is $\approx 10^{-2}\text{–}10^{-6}$. The saturation roughness [Fig. 3(b)] reaches a maximum value at 125 °C, and increases rapidly when the transition from grains to lamellae occurs. Although the number of samples does not allow us to assess the trend unambiguously, it is interesting that the surface roughness exhibits a pretransitional smoothing that should appear in the optical and electrical properties of the interface.

The self-affine part of the spectrum spans one order of magnitude of the spatial frequencies at 25 °C and reaches about 3 orders of magnitude above 200 °C (Fig. 2). The roughness exponent α in Fig. 4 decays with temperature from about 1 at room temperature down to 0.7 at 200 °C. Thus, α maps the range within the predictions of diffusion-limited aggregation ($\alpha = 1$ [19]) and molecular-beam epitaxy (MBE) growth controlled by adsorption at kink sites ($\alpha = 0.66$ [20]). Similar values have been measured on amorphous films [10] and epitaxial growth [6(a)], respectively. $\alpha > 1$ indicates strongly correlated fluctuations due to features large with respect to the scale length [19], and has been reported in the early stages of faceted growth [6(b)]. In our system, the apparent scaling behavior exhibits a crossover from linear (diffusion) to nonlinear (adsorption) regimes. Since desorption of T6 is substantial above 250°, one might expect [1(a)] that at higher deposition T the exponent α would decrease further due to the onset of nonconservative mechanisms of growth [21]. The decrease of α with increasing T suggests the onset of a roughening transition [22], which has been predicted by discrete simulations [2] and nonlinear continuum theories of nonequilibrium growth [3]. In the restricted

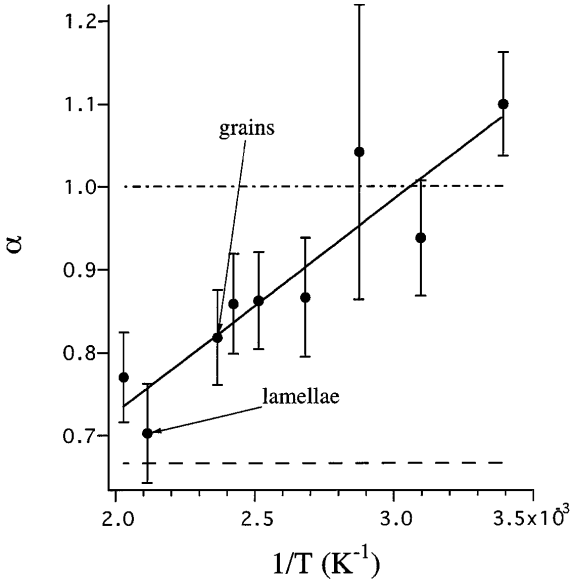

FIG. 4. Roughness scaling exponent α vs inverse temperature. Weighted best-fit line is $\alpha = 0.3(\pm 0.1) \pm 2.3(\pm 0.5) \times 10^{-2}/T(\mathrm{K})$ (solid line). Horizontal lines are the predictions of diffusional model (dot-dashed line) [19], and MBE growth (dashed line) [20]. Error bars represent the amount that the slope changes when the fitting in Fig. 2 is done on a larger frequency range.

solid-on-solid (RSOS) model [2] α saturates to a smaller value (0.25) for a deposition temperature (rescaled by the strength of the nearest-neighbor interaction) $1/\kappa \ll 1/\kappa_c \approx 2$. An apparent transition from amorphous to layered growth can be the consequence of a pretransitional macroscopic faceting [3]. In terms of α our system does not strictly fit into any of these pictures, and this opens the question of whether the anisotropy of the intermolecular potential can affect the growth mechanism. Interestingly, the rate of change of α (≈ 0.02 eV) with T is comparable to the strength of the van der Waals interaction $\varepsilon = 0.037$ eV between thienyl units on adjacent T6 molecules [17], and the transition occurs at $T \approx 200\,^{\circ}\mathrm{C} \approx 0.04$ eV. The analogy with Ref. [2] suggests that the relative mismatch between thienyl groups in adjacent molecules might be at the origin of the surface roughness. A small translation of a T6 molecule in the lattice along the direction of the major axis (which almost coincides with the crystallographic a axis [18]) would be thermally accessible and result in the breakdown of the ordered molecular arrangement.

Our tentative interpretation is that at low temperature (grain aggregation) diffusion is the rate limiting factor, and the mechanism of growth is changed with continuity to MBE (lamellae) as the mobility of the molecules increases at high T. Diffusion in the low-T range is consistent with the mechanism that was inferred from the evolution of the grain size distributions [17]. On mica, T6 molecules tend to nucleate normal to the surface [(100) contact plane]. As the mobility on the T6 surface increases on the (100) plane, the molecules can reach the terrace edges and be steadily adsorbed due to the strong side-by-side intermolecular interactions between T6 molecules. Thus, the adsorption on the (120) facets drives the lamellar growth.

Finally, we want to emphasize that the long-range order within the single domains and the smoothness of the interface exhibit opposite trends with substrate temperature. Since basic physical processes in these films involve transport and interface phenomena, such as exciton migration, charge injection, and energy transfer, then the optoelectronic response should be tuned by controlling not only the molecular order but also the surface fluctuations. While carrier mobility is enhanced in high-temperature aggregates with large ordered domains [16], our results suggest that there will be increased percolation and higher local electric fields due to larger fluctuations of one of the metal-organic interfaces. The unbalanced injection of carriers will lower the space-charge limit threshold and consequently the electroluminescence yield.

We acknowledge P. Pasini, A. Stella, P. Viville, R. Lazzaroni, P. Ostoja, C. Taliani, and J. Krim for stimulating discussions. This work was supported by EC Human Capital Mobility Network SELMAT and Esprit Basic Research Project No. 8013 LEDFOS.

[1] (a) A.-L. Barabási and H. E. Stanley, *Fractal Concepts in Surface Growth* (Cambridge University Press, Cambridge, United Kingdom, 1995); (b) *Dynamics of Fractal Surfaces*, edited by F. Family and T. Vicsek (World Scientific, Singapore, 1991); (c) T. Halpin-Healy and Y.-C. Zhang, Phys. Rep. **254**, 215 (1995); (d) P. Meakin, Phys. Rep. **235**, 189 (1993); (e) Y.-C. Yang, T.-M. Lu, and G.-C. Wang, *Diffraction from Rough Surfaces and Dynamic Growth Fronts* (World Scientific, Singapore, 1993).
[2] J. Amar and F. Family, Phys. Rev. Lett. **64**, 543 (1990).
[3] T. Hwa, M. Kardar, and M. Paczuski, Phys. Rev. Lett. **66**, 441 (1991).
[4] R. Chiarello, V. Panella, and J. Krim, Phys. Rev. Lett. **67**, 24 (1991).
[5] W. Weber and B. Lengeler, Phys. Rev. B **46**, 7953 (1992).
[6] (a) Y.-L. He, H.-N. Yang, T.-M. Lu, and G.-C. Wang, Phys. Rev. Lett. **69**, 3770 (1992); (b) K. Fang, T.-M. Lu, and G.-C. Wang, Phys. Rev. B **49**, 8331 (1994).
[7] Ph. Dumas, B. Bouffakhredine, C. Amra, O. Vatel, E. Andre, R. Galindo, and F. Salvan, Europhys. Lett. **22**, 717 (1993).
[8] J. Krim, I. Heyvaert, C. V. Haesendonck, and Y. Bruynseraede, Phys. Rev. Lett. **70**, 57 (1993).
[9] (a) J. M. Gómez-Rodríguez, A. M. Baró, L. Vázquez, R. C. Salvarezza, J. M. Vara, and A. J. Arvia, J. Phys. Chem. **96**, 347 (1992); (b) L. Vázquez, R. C. Salvarezza, P. Ocón, P. Herrasti, J. M. Vara, and A. J. Arvia, Phys. Rev. E **49**, 1507 (1994).
[10] H.-N. Yang, Y.-P. Zhao, G.-C. Wang, and T.-M. Lu, Phys. Rev. Lett. **76**, 3774 (1996).
[11] M. W. Mitchell and D. A. Bonnell, J. Mater. Res. **5**, 2244 (1990).
[12] C. Douketis, H. Z. Whang, T. L. Haslett, and M. Moskovits, Phys. Rev. B **51**, 11 022 (1995).
[13] G. W. Collins, S. A. Letts, E. M. Fearon, R. L. McEachern, and T. P. Bernat, Phys. Rev. Lett. **73**, 708 (1994).
[14] P. Ocón, P. Herrasti, J. M. Vara, L. Vázquez, R. C. Salvarezza, and A. J. Arvia, J. Phys. Chem. **98**, 2418 (1994).
[15] (a) H. Tada, K. Saiki, and A. Koma, Jpn. J. Appl. Phys. **30**, L306 (1991); (b) C. Ludwig, B. Gompf, W. Glatz, J. Petersen, W. Eisenmerger, M. Möbus, U. Zimmermann, and N. Karl, Z. Phys. B **86**, 397 (1992); (c) S. R. Forrest, P. E. Burrows, E. I. Haskal, and F. F. So, Phys. Rev. B **49**, 11 309 (1994).
[16] L. Torsi, A. Dodalabapur, L. J. Rothberg, A. W. P. Fung, and H. E. Katz, Science **272**, 1462 (1996).
[17] F. Biscarini, R. Zamboni, P. Samorì, P. Ostoja, and C. Taliani, Phys. Rev. B **52**, 14 868 (1995).
[18] B. Servet, G. Horowitz, S. Ries, O. Lagorsse, P. Alnot, A. Yassar, F. Deloffre, P. Srivastava, R. Hajlaoui, P. Lang, and F. Garnier, Chem. Mater. **6**, 1809 (1994).
[19] D. E. Wolf and J. Villain, Europhys. Lett. **13**, 389 (1990).
[20] Z.-W. Lai and S. Das Sarma, Phys. Rev. Lett. **66**, 2348 (1991).
[21] M. Kardar, G. Parisi, and Y.-C. Zhang, Phys. Rev. Lett. **56**, 889 (1986).
[22] Y.-C. Yang, T.-M. Lu, and G.-C. Wang, Phys. Rev. Lett. **63**, 1621 (1989).